

Theoretical Characteristics of Deactivated Lichens Fixed Bed Column for the Crystal Violet and Methyl Red Dyes Adsorption

Kouassi Kouadio Dobi-Brice¹, Ekou Lynda¹, Yacouba Zoungnan^{2,*}, Ekou Tchirioua¹

¹Basic and Applied Sciences Training and Research Unit, Department of Chemistry,
University Nangui Abrogoua 02 B.P. 801 Abidjan 02, Ivory Coast

²Biological Sciences Training and Research Unit, Department of Mathematics, Physics and Chemistry, University Peleforo Gon
Coulibaly. B.P. 1328, Korhogo, Ivory Coast

*Corresponding author: zoungnan@gmail.com

Received February 10, 2020; Revised March 12, 2020; Accepted March 24, 2020

Abstract Among the methods of wastewater treatment, adsorption is the one that remains accessible because it is easy to implement. It uses less expensive, abundant and available adsorbent supports. Adsorption can be implemented through two types of processes: continuous adsorption and discontinuous adsorption. Continuous adsorption allows the treatment of large volumes of water compared to discontinuous adsorption, which is suitable for the treatment of small quantities of water [1]. This study is part of an approach to the removal of toxic dyes using the continuous mode adsorption method. Two dyes were used: crystal violet and methyl red. The adsorbent fixed bed of the column consists of biomass of previously deactivated lichens. The influence of some physico-chemical parameters on the column such as flow rate, lichen grain size, adsorbent bed mass and initial dye concentration were evaluated. The application of Bohart-Adams, Thomas and Yonn-Nelson models to the experimental data made it possible to predict the theoretical characteristics of the column. For a given dye, under the influence of a given physico-chemical parameter, the application of the Bohart-Adams model determined the saturation concentration of the adsorbent bed (N_0). The application of the Thomas model allowed to determine the theoretical adsorption capacity of the column (Q_{the}), and the Yonn-Nelson model allowed to predict the time (τ) necessary for the 50% breakthrough of the adsorbent bed.

Keywords: wastewater, adsorption, column, lichens, models, dyes

Cite This Article: Kouassi Kouadio Dobi-Brice, Ekou Lynda, Yacouba Zoungnan, and Ekou Tchirioua, "Theoretical Characteristics of Deactivated Lichens Fixed Bed Column for the Crystal Violet and Methyl Red Dyes Adsorption." *American Journal of Water Resources*, vol. 8, no. 2 (2020): 69-77. doi: 10.12691/ajwr-8-2-3.

1. Introduction

In recent years, Côte d'Ivoire has developed an industrial expansion, particularly in the plastic, rubber, wood, agro-industry, petrochemical, cosmetics, leather, paper and textile sectors [2,3]. These industries use various dyes in their operations. Unfortunately, only 1% of these industries have effluent treatment plants [3]. The effluents of most of these industrial units are thus discharged into the environment without any prior treatment. However, some of dyes contained in these waste waters are sometimes toxic or even carcinogenic to humans and also have harmful effects on the environment [4]. Water pollution by dyes from these industrial effluents has therefore become a health and environmental problem. Numerous studies have focused on industrial wastewater treatment methods. Among these methods are electrochemical oxidation [5], ozonation [6], electrocoagulation [7], Fenton photo process [8], nanofiltration, reverse osmosis [9], etc.

Some of these methods are expensive and inefficient for treating wastewater containing dyes. Several studies have revealed the limitations of these methods related to the production of toxic by-products [10,11]. This has led the scientific community to move towards alternatives such as the adsorption method. Adsorption media can be natural or artificial. However, the use of natural adsorbents such as clay [12], activated carbon [13], sawdust [14], peanut shells [15], orange peel [16] and banana peels [17] remains the cheapest and easiest to use. It is in this context that the present study was carried out with the aim of removing crystal violet (CV) and methyl red (MR), two toxic dyes, through a continuous adsorption column. The fixed bed of the column is a biomass of lichens. Lichens are plant species that result from the symbiotic association between an alga and a fungus. Lichens have been used as sorbents in several pollutant removal studies such as metallic trace elements [18-24]. However, there are few studies on dye removal by continuous adsorption using lichens as an adsorbent bed. This study will more specifically determine the theoretical characteristics of the

proposed adsorption column. To do so, the Bohart-Adams, Thomas and Yonn-Nelson models were applied to the results of the evaluation of the influence of physico-chemical parameters such as flow rate, lichen grain size, lichen mass and initial dye concentration.

2. Material and Methods

2.1. Sampling

The thalli of the lichen *Parmotrema dilatatum* were collected in the forest reserve of the LAMTO ecological station (5.02 °C West and 6.13 °C North). This reserve is 174 km far from the city of Abidjan (Ivory Coast) and located on the Abidjan-Yamoussoukro axis, between Singrobo and Taabo, and stretches along the Bandama River. This space is a natural Park of 2500 ha, with a tropical climate, the average temperature per year is about 28.28 °C, the annual precipitation is around 1194 mm and the rate of humidity is higher than 58%.

Sampling is carried out on mature trees with diameters greater than 20 cm with bark that is not cracked, injured or slanted. Lichens collected are sent to the laboratory.

2.2. Lichens Deactivation and Crushing

In the laboratory, lichens are detached from their substrates and then manually cleaned to remove soil, leaf, dust or insect debris. The thallus is then washed with distilled water. An appropriate amount of lichen is placed in an oven at 80 °C for 48 hours to deactivate them. The deactivated lichens are crushed and sieved.

2.3. Dyes Preparation

Solutions of 500 mg/L of CV dye, and MR were prepared. We diluted the initial solutions in order to obtain diluted solutions.

The chemical structures and some characteristics of the dyes are given below (Figure 1).

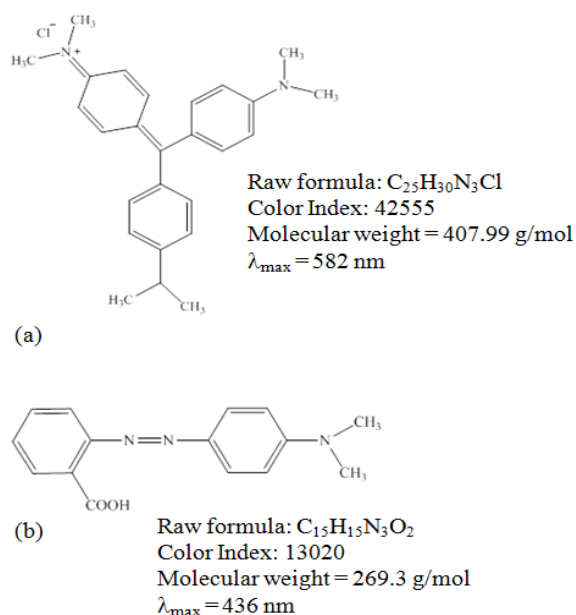


Figure 1. Chemical structures of CV (a) and MR (b)

2.4. Experimental Device

The experimental device consists of a glass column 22 cm long and 8 cm inside diameter, a flow and storage vessel for the solution to be treated equipped with a valve with adjustable flow rate. A pump ensures the circulation of the solution to be treated in the column. The column contains a filter and reads adsorbent. Another container allows the treated solution to be recovered at the column outlet. (Figure 2).

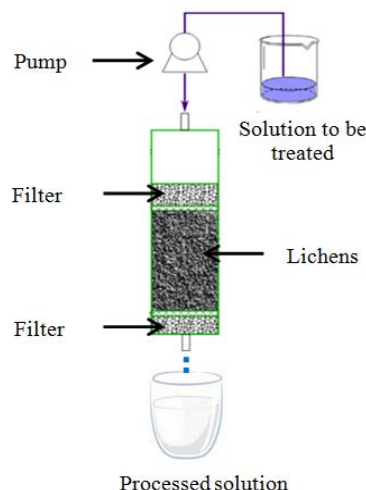


Figure 2. Photograph and diagram of the study device

2.5. Continuous Mode Adsorption Studies

The flow rate of the column was successively set at 0.07; 0.15 and 0.21 L/min. The effect of lichen grain size was examined using the grain sizes, [125 -250 μm], [250 -500 μm] and [500 -800 μm]. As for the influence of the height of the adsorption bed, the study was carried out by successively setting the lichen mass at 20, 40, 60, 80 and 100g. The effect of the initial concentration of dyes was studied between 10 and 30 mg/L. The optical density of the treated solution was read using a UV/visible spectrophotometer. The amount of dye adsorbed per gram of lichen at equilibrium Q_{exp} (mg/g) was calculated using the following relationship [25]:

$$Q_{\text{exp}} = \frac{DC_0 \int_0^{t_s} \left(1 - \frac{C_t}{C_0}\right) dt}{m} \quad (1)$$

Where:

C_0 is the initial concentration of the solute (mg/L),
 C_t the solute concentration (mg/L),

D flow rate (L/min),
 t_{total} the saturation time,
 m the lichen mass (g).

Q_{exp} is obtained by polynomial regression of Eq. (2), followed by its integration from $t = 0$ to $t = t_s$.

$$1 - \frac{C_t}{C_0} = f(t) \quad (2)$$

2.6. Models Description

The characteristics of the adsorption column were determined by applying numerical models. Knowledge of the theoretical characteristics of the column allows a better description of the different stages of the adsorption process and to know the temporal concentration profile between the liquid and solid phases [26]. The most recommended models are the Adams-Bohart, Thomas and Yoon-Nelson models [27]. Each of these models can be used to determine different operating parameters of the fixed-bed column.

2.6.1. Bohart-Adams Model

Bohart-Adams model [28] assumes that there is only one adsorption layer in dynamic regime. The adsorption equilibrium in this case is achieved on each grain of adsorbent and the reverse desorption reaction is possible. The Bohart-Adams model predicts the bed saturation concentration (N_0).

The Bohart-Adams model is given by the following expression:

$$\frac{C_t}{C_0} = \exp\left(k_{BA}C_0t - k_{BA}N_0\frac{z}{v}\right) \quad (3)$$

Where:

C_0 is the initial concentration of the solute (mg/L),
 C_t the solute concentration (mg/L),
 K_{BA} the kinetic constant of Bohart-Adams (L/mg.min),
 N_0 the saturation concentration of the bed (mg/L),
 v the flow rate of the solution (cm/min),
 z is the height of the adsorbent bed (cm).

The linear form of the Bohart-Adams model is given by the following relation [29]:

$$\ln\left(\frac{C_0}{C_t} - 1\right) = k_{BA}N_0\frac{z}{v} - k_{BA}C_0t \quad (4)$$

2.6.2. Thomas Model

Thomas model [30] assumes that the adsorption process follows pseudo-second-order kinetics, with no axial dispersion during flow in the adsorption column [31]. The Thomas model makes it possible to predict the theoretical adsorption capacity (Q_{the}) of the column. It is one of the most widely used models for the theoretical study of the performance of fixed bed adsorption columns.

Thomas model is given by the following expression:

$$\frac{C_t}{C_0} = \frac{1}{1 + \exp\left(\frac{k_{Th}Q_{\text{ads}}m}{D} - k_{Th}C_0t\right)} \quad (5)$$

Where:

C_0 is the initial concentration of the solute (mg/L),

C_t the solute concentration (mg/L),
 k_{Th} the Thomas constant (L.mg⁻¹.h⁻¹),
 m the mass of the adsorbent bed (g),
 Q_{the} the theoretical adsorption capacity (mg/g),
 D the flow rate (L.h⁻¹).

The linear form of this model is given by the expression:

$$\ln\left(\frac{C_0}{C_t} - 1\right) = \frac{k_{Th}Q_{\text{the}}m}{D} - k_{Th}C_0t. \quad (6)$$

2.6.3. Yoon-Nelson Model

Yoon-Nelson model [32] provides information on the time τ the required for 50% saturation of the column bed.

The Yoon-Nelson model takes the following form:

$$\frac{C_t}{C_0} = 1 + \exp(\tau k_{YN} - k_{YN}t) \quad (7)$$

Where:

C_0 is the initial solute concentration (mg/L),
 C_t the solute concentration (mg/L),
 k_{YN} the Yoon-Nelson kinetic constant (min⁻¹),
 τ the required for 50% saturation of the column bed.

The linearized form is given by the expression:

$$\ln\left(\frac{C_0}{C_t} - 1\right) = -k_{YN}C_0t + \tau k_{YN}. \quad (8)$$

These three numerical models have in common the expression:

$$\ln\left(\frac{C_0}{C_t} - 1\right) = f(t). \quad (9)$$

The function $f(t)$ is specific to each model. The linear regression obtained from this expression makes it possible to determine the different parameters of each model. Among these parameters are the theoretical characteristics of the column.

2.7. Data Processing

Data analysis and linear regressions were performed alternately using Microsoft Excel 2010 software and STATISTICA 8.0.360.0.

3. Results and Discussion

3.1. Influence of the Flow Rate

The linear regressions of Eq. (9) obtained from the experimental results of the influence of dye flow through the fixed-bed column are shown in Figure 3.

The parameters of the Bohart-Adams, Thomas and Yoon-Nelson model relating to the study of the influence of the dye flow through the fixed bed column of deactivated lichens are recorded in Table 1.

3.1.1. Bohart-Adams model

For each dye, increasing the flow rate from 0.07 to 0.21 L/min, results in an increase in the Bohart-Adams speed constant (k_{BA}). The bed saturation concentration (N_0)

decreases as the flow rate of the dye through the column increases. The highest values of the Bohart-Adams velocity constant (k_{BA}) are $15.1 \cdot 10^{-4}$ for CV and $35 \cdot 10^{-4}$ L/(mg.min) for MR. These velocity constants are obtained at the lowest flow rate ($D = 0.07$ L/min) with high correlation coefficients. The increase with flow of the constant k_{BA} , also called mass transfer coefficient, reflects the fact that the overall kinetics of the system is dominated by the mass transfer in the initial part of the bed of the column [33]. In their studies of phenol adsorption on a fixed-bed column of polymer resins, [34] also found that increasing flow rate increased the k_{BA} constant but, contrary to our results, they observed an increase in the N_0 saturation concentration of the bed with increasing flow rate. However, [35] in their work on antibiotic adsorption on a fixed bed column, showed that a low flow rate increased the bed saturation concentration (N_0) and decreased the Bohart-Adams k_{BA} rate constant.

3.1.2. Thomas Model

The results in Table 1 show that the theoretical (Q_{the}) and experimental (Q_{exp}) adsorption capacities increase with the decrease in the flow rate of the dyes in the column. The Q_{the} values estimated by Thomas' model are close to Q_{exp} . The experimental data of the study are therefore well described by Thomas' model. Thus, with the flow rate $D = 0.07$ L/min, the quantities of CV and MR experimentally adsorbed are 14.29 and 8.87 mg/g respectively. Theoretically with the same flow rate, the quantities obtained are 14.52 mg/g for CV and 9.16 mg/g for MR. Whatever the dye, the values of the kinetic constant Thomas (k_{Th}) decrease with increasing flow rate. The same is true for the theoretical adsorption capacity. The high Q_{the} value at low flow rates is due to the slow contact, which promotes the diffusion [36] of the dyes into

the column bed. Conversely, the low Q_{the} value at high flow rate is due to insufficient diffusion of the dye molecules [37]. The good description of the experimental data by Thomas' model reveals that the adsorption process of the studied dyes follows second order kinetics [38]. The authors [33] studying the removal of antibiotics on a fixed bed column also observed that the increase in flow rate induced a decrease in the theoretical adsorption capacity and an increase in the Thomas constant. The Thomas model was also used by [34] in a fixed-bed column study. They found that the Thomas constant depended on the flow rate and that the theoretical amount of adsorption increased with decreasing flow rate.

3.1.3. Yoon-Nelson Model

The values of the Yoon-Nelson velocity constant (k_{YN}), the time (τ) required for 50% saturation of the column bed and the coefficient of determination are recorded in Table 1. For each dye, the k_{YN} values increase with increasing flow rate, while the time required for 50% saturation of the column bed decreases. Thus, for a flow rate of 0.07 to 0.21 L/min, k_{YN} increased from $55 \cdot 10^{-4}$ to $55.1 \cdot 10^{-3} \text{ min}^{-1}$ for CV and from $83 \cdot 10^{-4}$ to $35 \cdot 10^{-3}$ for MR. The time (τ) has increased from 1244.26 to 243.18 min for CV and 785.23 to 131.85 for MR. The decrease of the Yoon-Nelson velocity constant reflects the negative effect of the increased flow rate on the adsorption capacity [39]. Similarly, the time required to reach 50% bed saturation decreases with increasing column throughput due to the faster saturation of the bed [40]. A similar trend was observed by [41] in a study on the adsorption of amoxicillin in a fixed bed of activated carbon. Other authors [42] have also reported similar observations in simulated atenolol-carbon system failure data [43].

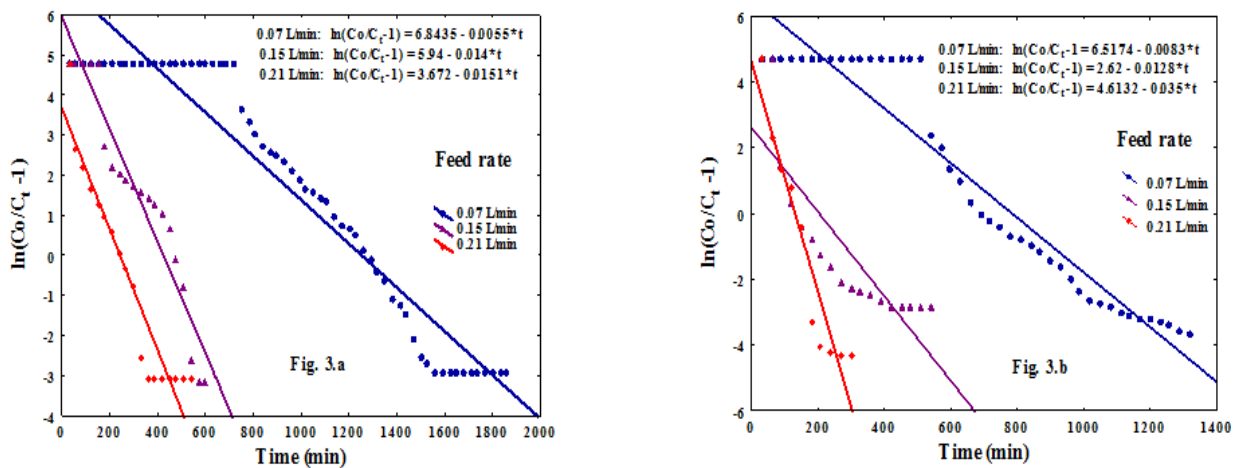


Figure 3. Influence of the column flow rate: Crisol Violet (a) and Methyl Red (b)

Table 1. Models parameters relating to the influence of the flow rate for the absorption of CV and MR

Dyes	Flow rate (L/min)	Bohart-Adams			Q_{exp} (mg/g)	Thomas			Yoon-Nelson		
		N_0 (mg/L)	k_{BA} (L/mg.min)	r^2		Q_{the} (mg/g)	k_{Th} (L/mg.min)	r^2	τ (min)	k_{YN} (min^{-1})	r^2
CV	0.07	4331.95	$55 \cdot 10^{-5}$	0.922	14.29	14.52	$55 \cdot 10^{-5}$	0.922	1244.26	$55 \cdot 10^{-4}$	0.922
	0.15	3165.34	$14 \cdot 10^{-4}$	0.922	10.18	10.61	$14 \cdot 10^{-4}$	0.922	424.286	$14 \cdot 10^{-3}$	0.922
	0.21	2539.89	$15 \cdot 10^{-4}$	0.909	7.59	8.511	$15 \cdot 10^{-4}$	0.909	243.179	$15 \cdot 10^{-3}$	0.909
MR	0.07	27333.8	$83 \cdot 10^{-5}$	0.925	8.87	9.161	$83 \cdot 10^{-5}$	0.925	785.229	$83 \cdot 10^{-4}$	0.925
	0.15	1527.05	$12.8 \cdot 10^{-4}$	0.724	4.75	5.117	$12.8 \cdot 10^{-4}$	0.724	204.688	$12.8 \cdot 10^{-3}$	0.724
	0.21	1376.65	$35 \cdot 10^{-4}$	0.914	3.79	4.613	$35 \cdot 10^{-4}$	0.914	131.806	$35 \cdot 10^{-3}$	0.914

3.2. Influence of Particle Size

Linear regressions of Eq. (9) obtained from the experimental results of the influence of lichen grain size in CV and RM adsorptions are presented in Figure 3.

Table 2 combines the Bohart-Adams, Thomas and Yoon-Nelson model parameters for studying the influence of lichen grain size on dye adsorption through the fixed-bed column.

3.2.1. Bohart-Adams Model

The results recorded in Table 2 show that the fixed bed saturation concentration (N_0) decreases with increasing lichen grain size. However, the Bohart-Adams Velocity Constant (k_{BA}) increases with increasing lichen particle size. For grain size [125-250 μm], N_0 increased from 4331.95 to 2975.08 L/(mg.min) for CV and from 2733.78 to 2111.62 mg/L for MR. The high values of the Bohart-Adams constant (k_{BA}) in the same grain size interval are $71 \cdot 10^{-4}$ L/(mg.min) for CV and $12 \cdot 10^{-4}$ L/(mg.min) with MR. The Bohart-Adams model is therefore perfectly described with small lichen grain sizes.

3.2.2. Thomas Model

According to Table 2, the theoretical and experimental adsorption capacity values decrease as the grain size of the lichens that make up the fixed bed in the adsorption column increases. However, Thomas' kinetic constant increases with the diameter of the deactivated lichen grains. The values of the theoretical adsorption capacities (Q_{the}) predicted by Thomas' model are close to those obtained experimentally (Q_{exp}). Indeed, with lichen grain

sizes between [125-250 μm]; [250-500 μm] and [500-800 μm]; the theoretical quantities of CV adsorption on the fixed bed are respectively 14.52, 13.42 and 9.98 mg/g while those obtained experimentally are 14.29, 13.35 and 9.83 mg/g. The values of the Thomas k_{Th} kinetic constant in CV adsorption range from $55 \cdot 10^{-5}$ to $71 \cdot 10^{-5}$ L/(mg.min) respectively with grain sizes from 125 μm to 800 μm . For MR, k_{Th} increases from $83 \cdot 10^{-5}$ to $12 \cdot 10^{-4}$ L/(mg.min). The good agreement between the experimental adsorption capacities and those theoretically predicted by Thomas' model shows that adsorption follows second-order kinetics [38].

3.2.3. Yoon-Nelson Model

Analysis of the Yoon-Nelson model parameter values reported in Table 2, shows that lichen particle size influences the time τ , required for 50% saturation of the column bed. Particle size also influences the Yoon-Nelson kinetic constant (k_{YN}). An increase in grain size leads to a decrease in time τ and an increase in k_{YN} . When grain size varies from 125 μm to 800 μm , the time τ , drops from 883.58 min to 529.67 min with CV. For MR the time τ drops from 785.23 min to 606.53 min. The k_{YN} constant in the case of CV adsorption went from $55 \cdot 10^{-4}$ to $71 \cdot 10^{-4}$ L/(mg.min) and from $83 \cdot 10^{-4}$ to $12 \cdot 10^{-3}$ L/(mg.min) in the case of MR. The k_{YN} constant therefore increases with lichen grain size while time τ decreases. This can be explained by the fact that with small grain sizes there is a reduction in the diffusion path [43] of the dye in the matrix. However, the authors [44] in a study on the adsorption of ionic liquids through an activated carbon fixed bed column, observed high k_{YN} values with small activated carbon grain sizes.

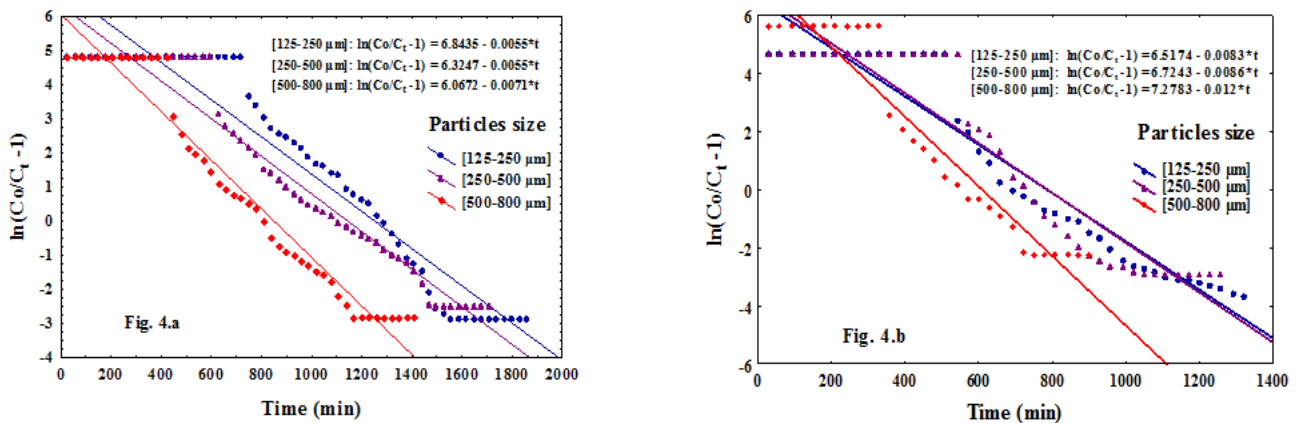


Figure 4. Influence of deactivated lichens particles size: Cristal Violet (a) and Methyl Red (b)

Table 2. Parameters of models under the influence of lichen grain size

Colorants	Granulométrie (μm)	Bohart-Adams			Thomas			Yoon-Nelson			
		N_0 (mg/L)	k_{BA} (L/mg.min)	r^2	Q_{exp} (mg/g)	Q_{the} (mg/g)	k_{Th} (L/mg.min)	r^2	τ (min)	k_{YN} (min^{-1})	r^2
CV	[125-250]	4331.95	$55 \cdot 10^{-5}$	0.922	14.29	14.52	$55 \cdot 10^{-5}$	0.922	1244.27	$55 \cdot 10^{-4}$	0.922
	[250-500]	4003.35	$55 \cdot 10^{-5}$	0.95	13.35	13.42	$55 \cdot 10^{-5}$	0.95	1149.95	$55 \cdot 10^{-4}$	0.95
	[500-800]	2975.08	$71 \cdot 10^{-5}$	0.955	9.83	9.977	$71 \cdot 10^{-5}$	0.955	854.535	$71 \cdot 10^{-4}$	0.955
MR	[125-250]	2733.78	$83 \cdot 10^{-5}$	0.925	8.87	9.161	$83 \cdot 10^{-5}$	0.925	785.229	$83 \cdot 10^{-4}$	0.925
	[250-500]	2722.18	$86 \cdot 10^{-5}$	0.891	8.56	9.122	$86 \cdot 10^{-5}$	0.891	781.895	$86 \cdot 10^{-4}$	0.891
	[500-800]	2111.62	$12 \cdot 10^{-4}$	0.925	6.68	7.076	$12 \cdot 10^{-4}$	0.925	606.525	$12 \cdot 10^{-3}$	0.925

3.3. Influence of Column Bed Mass

The linear regressions of Eq. (9), obtained from the experimental results of the influence of lichen mass in the adsorption of dyes through the fixed-bed column, are shown in Figure 5.

The parameter values of the Bohart-Adams, Thomas and Yoon-nelson models determined from the study of the influence of the lichen mass, constituting the fixed bed of the column, are shown in Table 3.

3.3.1. Bohart-Adams Model

The saturation concentration (N_0) of the bed and the kinetic constant (k_{AB}) are recorded in Table 3. The saturation concentration increases with the mass of the adsorbent bed. The kinetic constant (k_{BA}) decreases with increasing lichen mass in the column. Thus, for CV, the saturation concentration increased from 2984.39 to 6362.67 mg/L for a mass change of 40 to 100g of deactivated lichens. For MR, the N_0 increased from 1893.15 mg/L to 4351.05 mg/L. The increase in the mass of the adsorbent bed resulted in a decrease in the kinetic constant k_{BA} from $10.4 \cdot 10^{-4}$ to $17 \cdot 10^{-5}$ L/ (mg.min) for CV and from $15 \cdot 10^{-4}$ to $27 \cdot 10^{-5}$ L/ (mg.min) for MR. The authors [34] applied the Bohart-Adams adsorption model

to describe the adsorption of phenol on polymer resins in a fixed-bed column. They also found that the saturation concentration (N_0) decreased as the mass of the adsorbent bed increased. However, they observed an increase in the k_{BA} constant with increasing adsorbent bed mass.

3.3.2. Thomas Model

Analysis of the values in Table 3, obtained by application of Thomas' model, shows that the theoretical (Q_{the}) and experimental (Q_{exp}) adsorption capacities of the CV and MR dyes are close and increase with the mass of the column bed. In the case of Q_{exp} , that of CV rose from 7.13 to 21.6 mg/g and that of MR from 4.75 to 17.33 mg/g. In the case of Q_{the} , it rose from 7.501 to 25.586 mg/g in the case of CV and from 4.758 to 17.497 mg/g in the case of MR. Table 3 further reveals that, as the adsorbent bed mass increases, Thomas' rate constant decreases. Such a trend was observed by [34] in the case of phenolic adsorption of vinasse wines on a fixed bed column of polymer resins. Other authors [45] also applied Thomas' model in the case of tetracycline adsorption in a modified silica fixed-bed column. They also found that the adsorption capacity increased and k_{Th} also decreased with the height of the column bed.

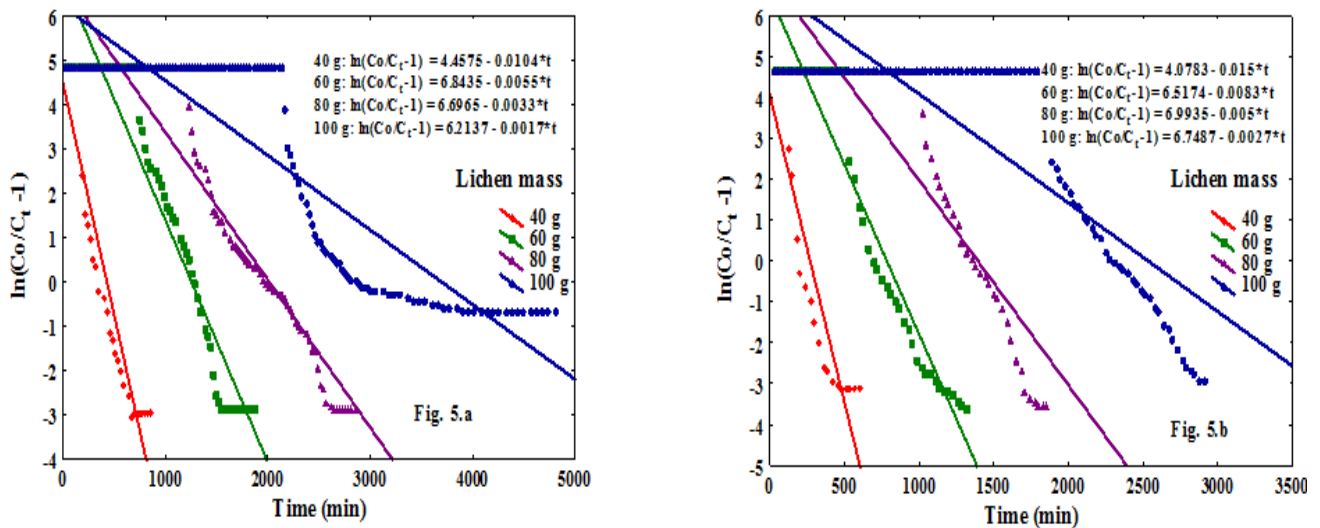


Figure 5. Influence of deactivated lichens mass: Cristal Violet (a) and Methyl Red (b)

Table 3. Parameters of models relating to different mass of deactivated lichens

Dyes	Lichen mass (g)	Bohart-Adams			Thomas			Yoon-Nelson			
		N_0 (mg/L)	k_{BA} (L/mg.min)	r^2	Q_{exp} (mg/g)	Q_{the} (mg/g)	k_{Th} (L/mg.min)	r^2	τ (min)	k_{YN} (min^{-1})	r^2
CV	40	2984.39	$10.4 \cdot 10^{-4}$	0.894	7.13	7.501	$10.4 \cdot 10^{-4}$	0.894	428.61	$10.4 \cdot 10^{-3}$	0.894
	60	4331.95	$55 \cdot 10^{-5}$	0.922	14.29	14.517	$55 \cdot 10^{-5}$	0.922	1244.3	$55 \cdot 10^{-4}$	0.922
	80	4709.89	$33 \cdot 10^{-5}$	0.918	17.12	17.756	$33 \cdot 10^{-5}$	0.918	2029.2	$33 \cdot 10^{-4}$	0.918
	100	6362.67	$17 \cdot 10^{-5}$	0.814	21.26	25.586	$17 \cdot 10^{-5}$	0.814	3655.1	$17 \cdot 10^{-4}$	0.814
MR	40	1893.15	$15 \cdot 10^{-4}$	0.852	4.75	4.758	$15 \cdot 10^{-4}$	0.852	271.89	$15 \cdot 10^{-3}$	0.852
	60	2733.78	$83 \cdot 10^{-5}$	0.925	8.87	9.161	$83 \cdot 10^{-5}$	0.925	785.23	$83 \cdot 10^{-4}$	0.925
	80	3246.39	$5 \cdot 10^{-5}$	0.828	12.16	12.239	$5 \cdot 10^{-5}$	0.828	1398.7	$5 \cdot 10^{-4}$	0.828
	100	4351.05	$27 \cdot 10^{-5}$	0.74	17.33	17.497	$27 \cdot 10^{-5}$	0.74	2499.5	$27 \cdot 10^{-4}$	0.74

3.3.3. Yoon-Nelson Model

Examination of Table 3 shows that the increase in the mass of the adsorbent bed induces an increase in the prediction time (τ) required for 50% saturation of the column bed and a decrease in the kinetic constant k_{YN} . Thus, considering a lichen mass varying from 40 to 100 g, the time τ increases from 428.61 to 3655.1 min in the case of CV treatment and from 271.89 to 2499.5 min in the case of MR. The variation in mass also leads to a decrease in the rate constant (k_{YN}) from $10.4 \cdot 10^{-3}$ to $17 \cdot 10^{-4}$ L/(mg.min) for CV treatment and from $15.4 \cdot 10^{-3}$ to $27 \cdot 10^{-4}$ L/(mg.min) for MR. The researchers [41] have recently applied the Yoon-Nelson model for the adsorption of amoxicillin on a fixed bed activated carbon column. The results of their work showed that the prediction time (τ) for 50% absorption of amoxicillin increased and that the Yoon-Nelson kinetic constant decreased with increasing bed height. The authors [34] in a study on the adsorption of phenol through a fixed bed column of polymer resins also observed an increase in time (τ) and a decrease in k_{YN} with increasing mass of the adsorbent, constituting the fixed bed of the column.

3.4. Influence of Dyes Concentration

Figure 6 shows linear regressions of Eq. (9) obtained from the experimental results of the influence of the initial dye concentration on lichen adsorption capacity.

Table 4 groups the parameters of the Bohart-Adams, Thomas and Yonn-Nelson models from the study of the influence of initial dye concentration.

3.4.1. Bohart-Adams Model

Values of Bohart-Adams model parameters in the removal of CV and MR at different initial concentrations are presented in Table 4. Analysis of these values shows that increasing dye concentration affects the bed saturation concentration (N_0) and the Bohart-Adams kinetic constant (k_{BA}). N_0 increases with increasing dye concentrations, while k_{BA} decreases. Thus, a change in CV concentration from 10 to 30 mg/L resulted in an increase in N_0 from 4331.95 to 5641.25 mg/L. As for MR, a change in concentration from 10 to 30 mg/L increased N_0 from 2733.78 to 4595.47 mg/L. The authors [35] applied the

Bohart-Adams model to the adsorption of two drugs (tetracycline and chloramphenicol) through a fixed-bed bamboo charcoal column. These authors reported that as the initial drug concentrations at the column inlet increased, N_0 also increased while k_{BA} decreased. Similarly, the authors [34], observed that the kinetic constant (k_{BA}) decreased with increasing phenol concentration and that the saturation concentration (N_0) also increased with the initial concentration.

3.4.2. Thomas Model

The values of the theoretical capacity (Q_{the}), the experimental capacity (Q_{exp}) and the Thomas' kinetic constant (k_{Th}) are contained in Table 4. From this table, it can be seen that, regardless of the dye, Q_{the} is close to Q_{exp} . The latter two parameters increase as the initial concentration of the dye increases; thus, for a change in initial dye concentration from 10 to 30 mg/L, Q_{exp} increases from 14.29 to 18.3 mg/g and Q_{the} increases from 14.52 to 18.9 mg/g for CV. For MR, Q_{exp} increases from 8.87 to 15.25 mg/g and Q_{the} increases from 9.16 to 15.4 mg/g. However, k_{Th} decreases with increasing initial dye concentration. A decrease in k_{Th} and an increase in Q_{the} and Q_{exp} with increasing initial dye concentrations can be explained by the fact that at lower concentrations the mass transfer is slower and thus improves the adsorption capacity [40]. A similar evolution of Q_{the} , Q_{exp} and k_{Th} was observed by [46] in a study of the adsorption of salicylic acid through a fixed bed column. These authors observed that k_{Th} values decreased while theoretical and experimental adsorption capacities increased with increasing initial salicylic acid concentrations.

3.4.3. Yoon-Nelson model

From the results in Table 4, it can be seen that increasing the initial dye concentration results in a reduction in the time (τ) required to saturate 50% of the column bed and an increase in the Yoon-Nelson kinetic constant (k_{YN}). The time (τ) is reduced from 1244.27 to 540.17 min in the treatment of CV and from 785.23 to 440.03 min in the case of MR, for an initial dye concentration ranging from 10 to 30 mg/L. As for (k_{YN}), it decreased from $55 \cdot 10^{-4}$ to $10.1 \cdot 10^{-3}$ L/(min.mg) for CV and from $83 \cdot 10^{-4}$ to $11.9 \cdot 10^{-3}$ L/(min.mg) for MR.

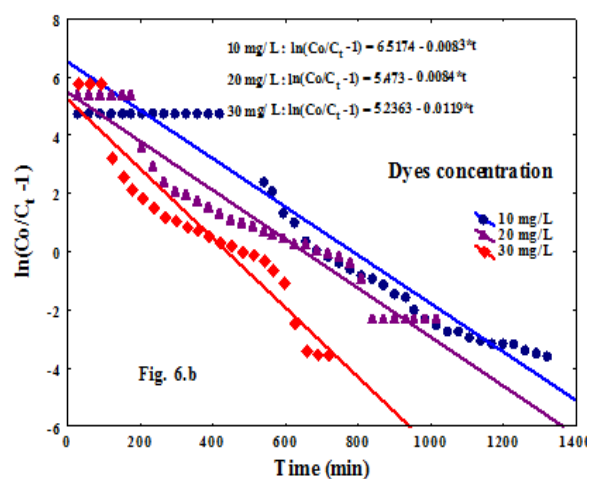
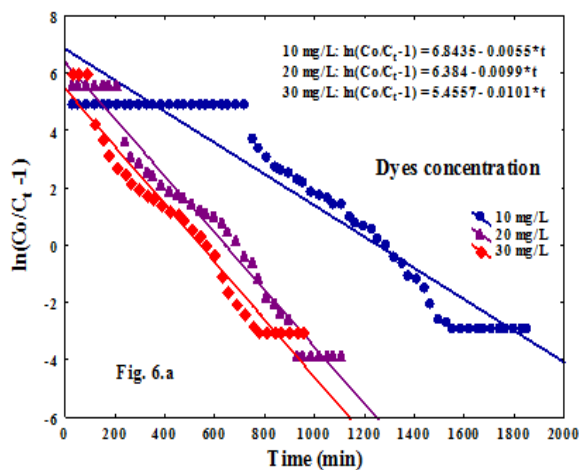


Figure 6. Influence of dyes concentration lichens mass: Cristal Violet (a) and Methyl Red (b)

Table 4. Parameters of models under influence of different initial concentrations in CV and MR

Dyes	Concentrations (mg/L)	Bohart-Adams			Thomas			Yoon-Nelson			
		N ₀ (mg/L)	k _{BA} (L/mg.min)	r ²	Q _{exp} (mg/g)	Q _{the} (mg/g)	k _{Th} (L/mg.min)	r ²	τ (min)	k _{YN} (min ⁻¹)	r ²
VC	10	4331.95	55*10 ⁻⁵	0.922	14.29	14.52	55*10 ⁻⁵	0.922	1244.27	55*10 ⁻⁴	0.922
	20	4490.1	49.5*10 ⁻⁵	0.974	14.65	15.05	49.5*10 ⁻⁵	0.974	644.848	49.5*10 ⁻⁴	0.974
	30	5641.25	33.67*10 ⁻⁵	0.96	18.3	18.9	33.67*10 ⁻⁵	0.96	540.168	33.7*10 ⁻⁴	0.96
MR	10	2733.78	83*10 ⁻⁵	0.925	8.87	9.161	83*10 ⁻⁵	0.925	785.229	83*10 ⁻⁴	0.925
	20	4536.74	42*10 ⁻⁵	0.941	14.73	15.2	42*10 ⁻⁵	0.941	651.548	42*10 ⁻⁴	0.941
	30	4595.47	39.67*10 ⁻⁵	0.912	15.25	15.4	39*67.10 ⁻⁵	0.912	440.025	39*7.10 ⁻⁴	0.912

The time (τ) decreases with increasing initial dye concentration due to faster saturation of the column bed [40]. The authors [41] applied the Yoon-Nelson model in the adsorption of amoxicillin through a fixed bed activated carbon column. The results of their study revealed that the time (τ) decreased while k_{YN} increased with increasing initial concentration of amoxicillin. Such trends were also observed by [47], in the fixed bed adsorption of doxycycline on an akagan-carbon composite; and by [48] in the fixed bed adsorption of ibuprofen on raspberry leaf charcoal.

4. Conclusion

This study made it possible to determine the theoretical characteristics of a column in the elimination of violet crystal and methyl red, by adsorption in continuous mode on a fixed bed of deactivated lichens. The parameters of the Bohart-Adams, Thomas and Yonn-Nelson models vary according to the dye flow rate in the column, the size of the lichen grains, the mass of the adsorbent bed and the initial concentration of dyes.

The theoretical characteristics obtained, that is to say, the saturation concentration (N_0) of the adsorbent bed, the theoretical adsorption capacity (Q_{the}) and the time (τ) required for 50% saturation of the column bed, are better at low dye flow rates. These theoretical characteristics are also better with the decrease in the size of lichen grains, the increase in the mass of the adsorbent bed and with high initial concentrations of dyes.

However, it would be interesting to determine these theoretical characteristics in a real industrial effluent treatment situation.

References

- [1] Piccin, J. S., Dotto, G. L., Vieira, M. L. G., "Kinetics and mechanism of the food dye FD&C red 40 adsorption onto chitosan.," *J Chem Eng Data*, 56, 3759-3765, 2011.
- [2] Houré A. A. E. and Tano A. P., "Politique économique et développement bilan diagnostic de l'industrie ivoirienne," Abidjan, Côte d'Ivoire, 2009.
- [3] Dongo, K. R., Niamke, B. F., Adje, A. F., Britton, B. G. H., Nama, L. A., Anoh, K. P., Adima, A. A. and Atta, K., "Impacts des effluents liquides industriels sur l'environnement urbain d'Abidjan-Côte D'Ivoire," *Int. J. Biol. Chem. Sci*, 7(1), 404-420, 2013.
- [4] Elmoubarki, R., Mahjoubi, F. Z., Tounsadi, H., Moustadraf, J., Abdennouri, M., Zouhri, A., El Albani, A. and Barka, N., "Adsorption of textile dyes on raw and decanted Moroccan clays: Kinetics, equilibrium and thermodynamics," *Water Resour. Ind.*, 9, 16-29, 2015.
- [5] Nidheesh, P. V., Zhou, M., and Oturan, M. A., "An overview on the removal of synthetic dyes from water by electrochemical advanced oxidation processes," *Chemosphere*, 197, 210-227, 2018.
- [6] Wijannarong, S., Aroonsrimorakot, S., Thavipoke, P., Kumsopa, C., and Sangjan, S., "Removal of Reactive Dyes from Textile Dyeing Industrial Effluent by Ozonation Process," *APCBEE Procedia*, 5, 279-282, 2013.
- [7] Pirkarami, A. and Olya, M. E., "Removal of dye from industrial wastewater with an emphasis on improving economic efficiency and degradation mechanism," *J. Saudi Chem. Soc.*, 21, S179-S186, 2017.
- [8] Sohrabi, M. R., Khavaran A., Shariati S., and Shariati S., "Removal of Carmoisine edible dye by Fenton and photo Fenton processes using Taguchi orthogonal array design," *Arab. J. Chem.*, 10, S3523-S3531, 2017.
- [9] Nataraj, S. K., Hosamani K. M., and Aminabhavi T. M., "Nanofiltration and reverse osmosis thin film composite membrane module for the removal of dye and salts from the simulated mixtures," *Desalination*, 249(1), 12-17, 2009.
- [10] Chaukura, N., Gwenzi W., Tavengwa N., and Manyuchi M. M., "Biosorbents for the removal of synthetic organics and emerging pollutants: Opportunities and challenges for developing countries," *Environ. Dev.*, 19, 84-89, 2016.
- [11] El-Aziz, A., Aref, A. M. A., El-Wahab, M. M. A. and Soliman A. S., "Application of Modified Bagasse as a Biosorbent for Reactive Dyes Removal from Industrial Wastewater," *J. Water Resour. Prot.*, 5, 10-17, 2013.
- [12] Kausar, A., Munawar, I., Anum, J., Kiran, A., Zill-i-Huma, N., Haq, N. B. and Shazia, N., "Dyes adsorption using clay and modified clay: A review," *J. Mol. Liq.*, 256, 395-407, 2018.
- [13] Baysal, M., Bilge, K., Yilmaz, B., Papila, M. and Yürüm, Y., "Preparation of high surface area activated carbon from waste-biomass of sunflower piths: Kinetics and equilibrium studies on the dye removal," *J. Environ. Chem. Eng.*, 6(2), 1702-1713, 2018.
- [14] Dulman, V. and Cucu-Man, S. M., "Sorption of some textile dyes by beech wood sawdust," *J. Hazard. Mater.*, 162(2-3), 1457-1464, 2009.
- [15] Liu, J., Wang, Z., Li, H., Hu, C., Raymer, P., and Huang, Q., "Effect of solid state fermentation of peanut shell on its dye adsorption performance," *Bioresour. Technol.*, 249, 307-314, 2018.
- [16] Arami, M., Limaee, N. Y., Mahmoodi, N. M. and Tabrizi, N. S., "Removal of dyes from colored textile wastewater by orange peel adsorbent: Equilibrium and kinetic studies," *J. Colloid Interface Sci.*, 288(2), 371-376, 2005.
- [17] Munagapati, V. S., Yarramuthi, V., Kim, Y., Lee, K. M. and Kim, D.-S., "Removal of anionic dyes (Reactive Black 5 and Congo Red) from aqueous solutions using Banana Peel Powder as an adsorbent," *Ecotoxicol. Environ. Saf.*, 148, 601-607, 2018.
- [18] Zounggran, Y., Ekou, L., Kouadio, K. and Brice, D., "Lichen Comme Bioindicateur de la Qualité de l'air de la Ville d'Abidjan en Éléments Traces Métalliques," *Eur. J. Sci. Res.*, 148(4), 501-511, 2018.
- [19] Ohnuki, T., Aoyagi, H., Kitatsuji, Y., Samadfam, M., Kimura Y., and William Purvis, O., "Plutonium(VI) accumulation and reduction by lichen biomass: correlation with U(VI)," *J. Environ. Radioact.*, 77(3), 339-353, 2004.
- [20] Uluozlu, O. D., Sari, A. and Tuzen, M., "Biosorption of antimony from aqueous solution by lichen (*Physcia tribacia*) biomass," *Chem. Eng. J.*, 163(3), 382-388, 2010.

- [21] Uluoğlu, O. D., Sari, A., Tuzen, M. and Soylak, M., "Biosorption of Pb(II) and Cr(III) from aqueous solution by lichen (*Parmelina tiliaceae*) biomass," *Bioresour. Technol.*, 99(8), 2972-2980, 2008.
- [22] Bingol, A., Aslan, A. and Cakici, A., "Biosorption of chromate anions from aqueous solution by a cationic surfactant-modified lichen (*Cladonia rangiformis* (L.)), " *J. Hazard. Mater.*, 161(2-3), 747-752, 2009.
- [23] Ekou, L., Zoungranan, Y., Ekou, T. and Kouadio, K. V. A., "Bioaccumulation Capacity of Cu and Fe on Lichen *Parmotrema Dilatatum*," *Eur. J. Sci. Res.*, vol. 145(3), 346-353, 2017.
- [24] Ekmekyapar, F., Aslan, A., Bayhan, Y. K. and Cakici, A., "Biosorption of copper(II) by nonliving lichen biomass of *Cladonia rangiformis* hoffm.," *J. Hazard. Mater.*, 137(1), 293-298, 2006.
- [25] Adrián Bonilla -Petriciolet; Didilia Ileana Mendoza -Castillo; Hilda Elizabeth Reynel -Ávila., *Adsorption Processes for Water Treatment and Purification*, Springer. México: Springer International Publishing, 2017.
- [26] De Franco, M. A. E., De Carvalho, C. B., Bonetto, M. M., Soares, R. de P. and Féris, L. A., "Removal of amoxicillin from water by adsorption onto activated carbon in batch process and fixed bed column: Kinetics, isotherms, experimental design and breakthrough curves modelling," *J. Clean. Prod.*, 161, 947-956, 2017.
- [27] Valenciano, R., Aylón, E. and Izquierdo, M. T. A., "A Critical Short Review of Equilibrium and Kinetic Adsorption Models for VOCs Breakthrough Curves Modelling." *J. Adsorption Science & Technology*, 33(10), 851-869, 2015.
- [28] Bohart, G. S. and Adams, E. Q., "Some aspects of the behavior of charcoal with respect to chlorine.," *J. Am. Chem. Soc.*, 42(3), 523-544, 1920.
- [29] Chu, K. H., "Fixed bed sorption: Setting the record straight on the Bohart-Adams and Thomas models," *J. Hazard. Mater.*, vol. 177, no. 1-3, pp. 1006-1012, May 2010.
- [30] Thomas, H. C., "Heterogeneous ion exchange in a flowing system.," *J Am Chem Soc.* 66, 1466-1664, 1944.
- [31] Wathukarage, A., Herath, I., Iqbal, M. C. M. and Vithanage, M., "Mechanistic understanding of crystal violet dye sorption by woody biochar: implications for wastewater treatment," *Environmental Geochemistry and Health*, 1-15, 2017.
- [32] Yoon Y. H. and Nelson J. H., "Application of gas adsorption kinetics: part 1: a theoretical model for respirator cartridge service time," *Am Ind Hyg Assoc J.*, 45, 509-516, 1984.
- [33] Lin, X. Li, R., Wen, Q., Wu, J., Fan, J., Jin, X., Qian, W., Liu, D., Chen, X., Chen, Y., Xie, J., Bai, J., and Ying, H "Experimental and modeling studies on the sorption breakthrough behaviors of butanol from aqueous solution in a fixed-bed of KA-I resin," *Biotechnol. Bioprocess Eng.*, 18(2), 223-233, 2013.
- [34] Soto, M. L., Moure, A., Domínguez, H. and Parajó, J. C., "Batch and fixed bed column studies on phenolic adsorption from wine vinasses by polymeric resins," *J. Food Eng.*, 209, 52-60, 2017.
- [35] Liao, P. Zhan, Z., Dai, J., Wu, X., Zhang, W., Wang, K. and Yuan, S., "Adsorption of tetracycline and chloramphenicol in aqueous solutions by bamboo charcoal: A batch and fixed-bed column study," *Chem. Eng. J.*, 228, 496-505, 2013.
- [36] Chen, N., Zhang, Z., Feng, C., Li, M., Chen, R., and Sugiura, N., "Investigations on the batch and fixed-bed column performance of fluoride adsorption by Kanuma mud," *Desalination*, 268(1-3), 76-82, 2011.
- [37] Kizito, S., Wu, S., Wandera, S. M., Guo, L. and Dong, R., "Evaluation of ammonium adsorption in biochar-fixed beds for treatment of anaerobically digested swine slurry: Experimental optimization and modeling," *Sci. Total Environ.*, 563-564, 1095-1104, 2016.
- [38] Zang, T. Cheng, Z., Lu, L., Jin, Y., Xu, X., Ding, W. and Qu, J., "Removal of Cr(VI) by modified and immobilized *Auricularia auricula* spent substrate in a fixed-bed column," *Ecol. Eng.*, 99, 358-365, 2017.
- [39] Xiang, H., Zhang, H., Liu, P. and Yan, Y., "Preparation of high purity propane from liquefied petroleum gas in a fixed bed by removal of sulfur and butanes," *Chem. Eng. J.*, 284, 224-232 2016.
- [40] Song, S.-T. Huan, Y.-F., Samana, N., Joharib, K., Cheua, S.-C., Konga, H. and Mat, H., "Process analysis of mercury adsorption onto chemically modified rice straw in a fixed-bed adsorber," *J. Environ. Chem. Eng.*, 4(2), 1685-1697, 2016.
- [41] Yaghmaeian, K., Moussavi, G. and Alahabadi, A., "Removal of amoxicillin from contaminated water using NH₄ Cl-activated carbon: Continuous flow fixed-bed adsorption and catalytic ozonation regeneration," *Chem. Eng. J.*, 236, 538-544, 2014.
- [42] Sancho, J. L. S., Rodríguez, A. R., Torrellas, S. Á. and Rodríguez, J. G., "Removal of an emerging pharmaceutical compound by adsorption in fixed bed column," *Desalin. Water Treat.*, 45, (1-3), 305-314, 2012.
- [43] Lemus, J., Moya, C., Gilarranz, M. A., Rodríguez, J. J. and Palomar, J., "Fixed-bed adsorption of ionic liquids onto activated carbon from aqueous phase," *J. Environ. Chem. Eng.*, vol. 5(6), 5347-5351, 2017.
- [44] Lemus, J., Palomar, J., Gilarranz, M. A. and Rodríguez, J. J., "On the Kinetics of Ionic Liquid Adsorption onto Activated Carbons from Aqueous Solution," *Ind. Eng. Chem. Res.*, 52(8), 2969-2976, 2013.
- [45] Liu, M., Hou, L., Yu, S., Xi, B., Zhao, Y., and Xia, X., "MCM-41 impregnated with A zeolite precursor: Synthesis, characterization and tetracycline antibiotics removal from aqueous solution," *Chem. Eng. J.*, 223, 678-687, 2013.
- [46] Meng, M. and al., "Highly efficient adsorption of salicylic acid from aqueous solution by wollastonite-based imprinted adsorbent: A fixed-bed column study," *Chem. Eng. J.*, 225, 331-339, 2013.
- [47] Zhang, X., Bai, B., Li Puma, G., Wang, H. and Suo, Y., "Novel sea buckthorn biocarbon SBC@β-FeOOH composites: Efficient removal of doxycycline in aqueous solution in a fixed-bed through synergistic adsorption and heterogeneous Fenton-like reaction," *Chem. Eng. J.*, 284, 698-707, 2016.
- [48] Dubey, S. P., Dwivedi, A. D., Lee, C., Kwon, Y.-N., Sillanpaa, M., and Ma, L. Q., "Raspberry derived mesoporous carbon-tubules and fixed-bed adsorption of pharmaceutical drugs," *J. Ind. Eng. Chem.*, 20(3), 1126-1132, 2014.

